Chapter 3

Experimental Setup and Methodology

3.1 Introduction

A wire explosion system with coaxial configuration has been built to conduct the study in this work. The system has been designed to facilitate the investigation of wire explosion in different ambient condition. Various diagnostic tools are also incorporated in the system. The focus of this work is to study the effect of different ambient condition on the powder characteristics as well as the wire explosion process.

The system being used in this work has four main parts. They have been summarized in Table 3.1. In sections 3.2 to 3.5, the major components in each part will be discussed. Meanwhile, the calculation of deposited energy in the wire will be described in sub-section 3.6.1. In section 3.7, the analyses of the powder by TEM, FESEM and XRD will be presented. The statistical study on the measured particle size will also be discussed.

Table 3.1: Main parts of the wire explosion system.

Parts	General functions	Major components
(a) Wire explosion circuit	Electrical circuit used to explode the wires.	(i) Charging unit and capacitor (ii) Spark gap switch (iii) Triggering unit (iv) Wire holders and wire (v) Chamber's body and Earth plate
(b) Powder collecting tools	Collect powder synthesized from the wire explosion process for characterization.	(i) Membrane filter (ii) Glass substrate (iii) Silicon substrate
(c) Gas and vacuum system	Evacuate vacuum chamber and supply gases to provide the required ambient condition.	(i) Gas cylinder and gas (ii) Rotary pump (iii) Pressure gauge (iv) Chamber
(d) Diagnostic tools	Record the current, voltage and radiation signals for the investigation of the wire explosion process.	(i) Magnetic pick-up coil and RC integrator (ii) High voltage probe (iii) PIN diode and biasing circuit

3.2 The wire explosion circuit

The equivalent circuit of the wire explosion circuit without the charging and triggering unit is shown in Figure 3.1. It is a LCR circuit where L_o is the circuit inductance without wire, L_w is the wire inductance, C is the capacitance while R_o and R_w are the circuit resistance without wire and the wire resistance respectively. A spark gap switch is used to control the discharge from the capacitor.

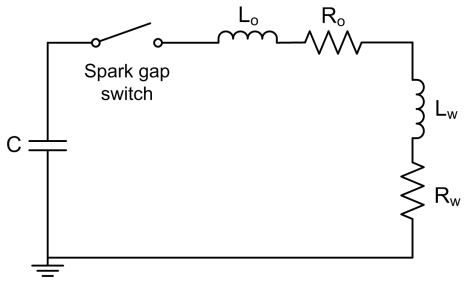

Figure 3.1: The wire explosion circuit without the charging and triggering units.

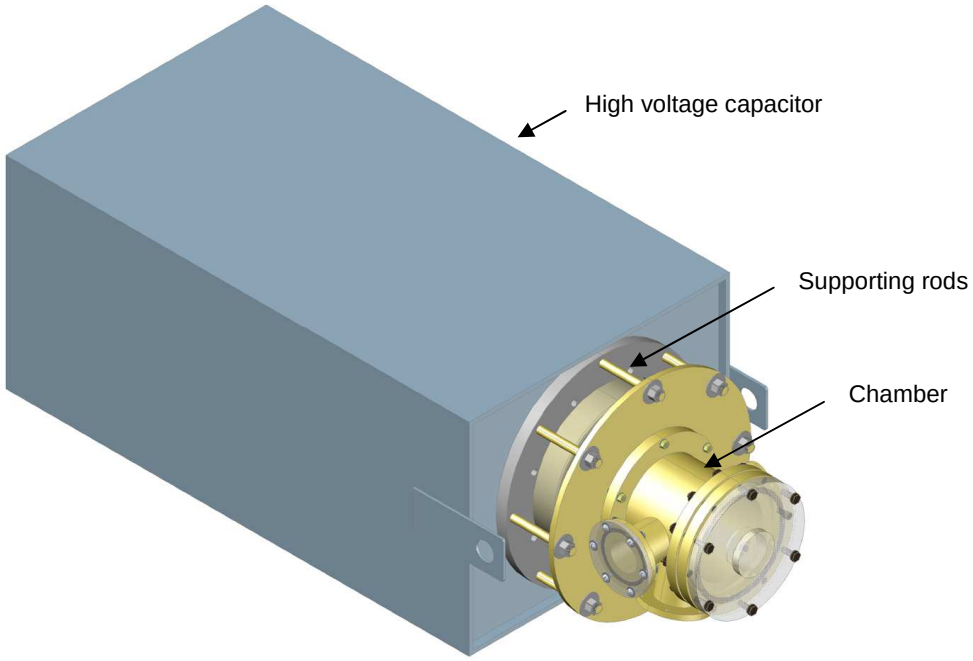

Figure 3.2: The 3D CAD diagram of the wire explosion circuit without the charging and triggering unit.

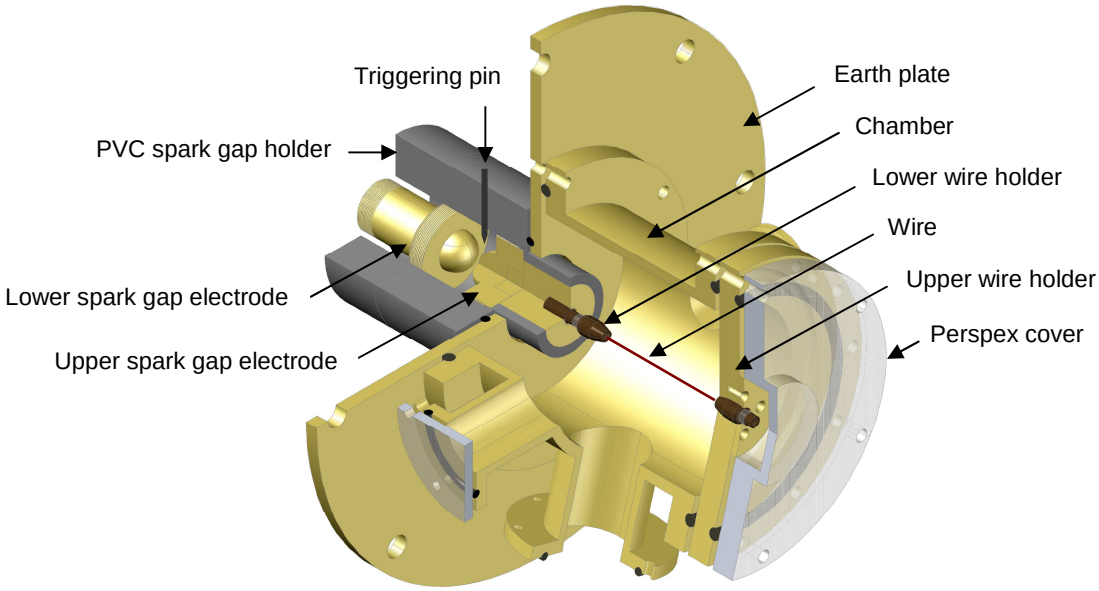

Figure 3.3: Enlarged cross-sectional view of the wire explosion circuit without capacitor, charging unit and triggering unit.

3.2.1 The charging unit and capacitor

The charging unit is formed by a high voltage transformer, a variac, a meter, a diode chain and a dumping switch. Its main function is to step up the voltage from the source and rectify the alternating voltage into a unipolar voltage. The unipolar voltage will be applied to the capacitor to charge it up to the required voltage. The circuit diagram of the charging unit is shown in Figure 3.4. A 1.85 µF Maxwell™ high voltage capacitor is used to generate the pulsed discharge current to explode the wire.

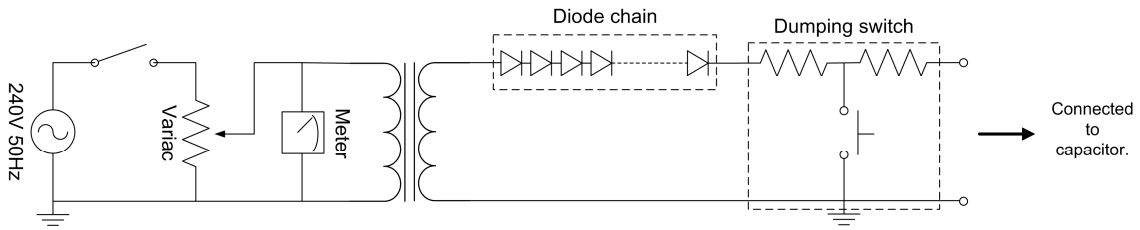

Figure 3.4: Circuit diagram of the charging unit.

3.2.2 Spark gap switch

The spark gap switch is shown in Figure 3.5. A symmetric spark gap is used as a switch to control the discharge from the capacitor. The lower spark gap electrode (main electrode) is directly connected to the capacitor. Meanwhile, the upper spark gap electrode is connected to the lower wire holder through a connector. In order to charge up the capacitor, the high voltage outlet of the charging unit is connected to the lower spark gap electrode that is attached to the high voltage charging point of the capacitor.

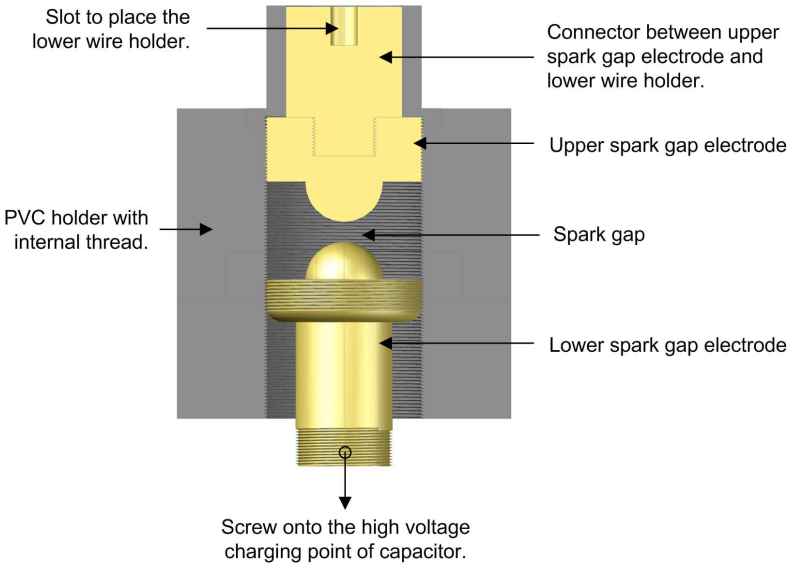

Figure 3.5: Components in the spark gap switch.

The gap spacing can be adjusted to vary the self-breakdown voltage of the switch. Since the ambient between the spark gap electrodes is air, the voltage required to cause a breakdown between the spark gap electrodes is approximately 3 kV per millimeter of gap distance.

3.2.3 Triggering unit

The triggering unit is used to trigger a breakdown across the spark gap such that a conducting path will be created across the gap. This will ‘close’ the spark gap switch and allow the current to flow into the wire from the capacitor. The triggering unit is formed by a triggering circuit, a step-up transformer, an isolating capacitor and a triggering pin. The position of the triggering pin is important to make a successful breakdown trigger of the spark gap. Detailed explanation can refer to (Bluhm, 2006).

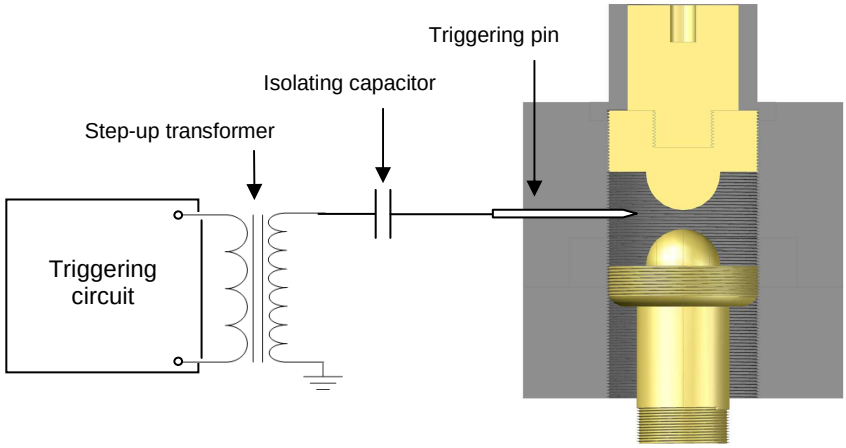

Figure 3.6: The triggering unit adapted to the spark gap.

3.2.4 Wire holders and wire

The wire holders are made of pin chuck where the wire will be clamped by the chuck when the chuck is closed. The pin chuck is shown in Figure 3.7.

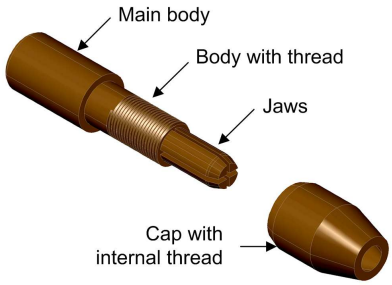

Figure 3.7: The pin chuck.

For the lower wire holder, the body of pin chuck has been plugged into the slot of the connector connected to the upper spark gap electrode as shown in Figure 3.3. On the other hand, the upper wire holder is formed by implanting a pin chuck at the center of a cylindrical brass plate (primary plate). The chuck is further secured at its position by another smaller secondary plate as shown in Figure 3.8. The cap of the chuck has been fixed at its position on the primary plate. The body of the chuck will be turned to open the chuck in this case.

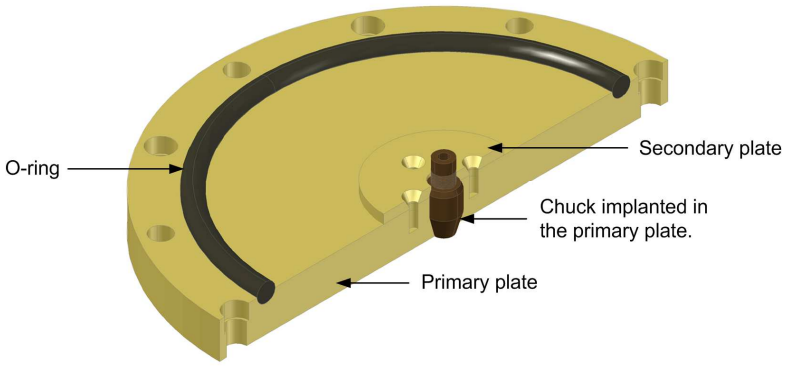

Figure 3.8: 3D cross-sectional view of upper wire holder.

Copper wires being used in the experiment have the specification as shown in Table 3.2. Length of the wire being exploded in each experiment is determined as the distance between the lower wire holder and the upper wire holder. It has been determined as 6.1 cm.

Table 3.2: Specification of copper wire.

1	Manufacturer	Goodfellow Cambridge Limited
2	Diameter	125 µm
3	Purity	99.9 %
4	Temper	Annealed

3.2.5 The chamber's body and Earth plate

The chamber's body is cylindrical in shape and has three cylindrical ports as shown in Figure 3.9. Port P1 as labeled in the figure is used as view port, P2 is connected to powder collecting mechanism while P3 is connected to vacuum and gas system. P1 and P2 have the same dimension while P3 has NW25 mount interface. Axis of P1 is aligned with the axis of P3 while axis of P2 is 75^{o} from axis of P1. A circular transparent Perspex plate is placed on P1 to close the port while enable observation into the chamber.

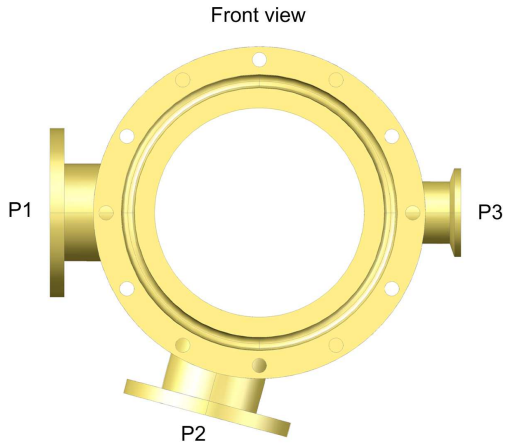

Figure 3.9: Front view of the chamber's body.

Earth plate is a circular brass plate with a diameter of 27.3 cm and a thickness of 0.65 cm. It is used as an adaptor between the chamber's body and the capacitor. It is known as Earth plate because it is electrically grounded through the connection to the capacitor casing that is connected to ground.

3.3 Powder collecting tools

Three powder collectors being used are membrane filter, silicon substrate and glass substrate. The membrane filter is used to collect the powder for TEM analysis. The membrane filter has a diameter of 2.5 cm and pore size of 15 nm. Meanwhile, silicon substrate and glass substrate are used to collect the powder for FESEM and XRD analysis respectively. The substrates are located at the bottom of the chamber to collect the powder.

The membrane filter system is shown in Figure 3.10. The system will collect the powder when the powder is forced to flow across the system. This is done by creating a pressure gradient across the system where the powder will move from the region of higher pressure to the region with lower pressure. A rotary pump is used to generate the pressure gradient.

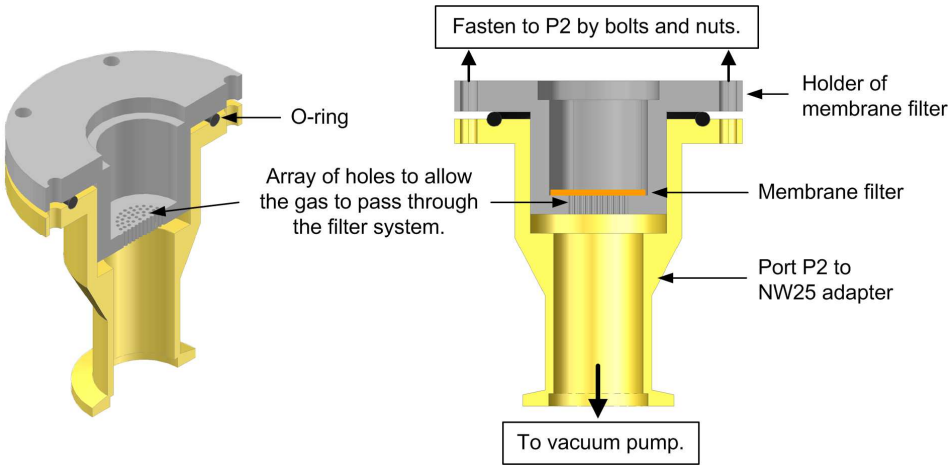

Figure 3.10: Cross-sectional view of the membrane filter system. (Left: 3D view; right: side view.)

3.4 Gas and vacuum system

The connection of the gas and vacuum system to the chamber is shown in Figure 3.11. Rotary pump is used to evacuate the chamber down to approximately 3 x 10^{-2} mbar while a capsule dial gauge is used to measure the pressure in the chamber. The chamber has been connected to the vacuum pump through two routes. They are called the upper evacuation route (upper route) and the lower evacuation route (lower route). The upper route is directly connecting the chamber to the vacuum pump while the particles filter system is located in the lower route. Two valves, namely, V1 and V2 have been located in each route to control the pumping process. Two gas cylinders consisted of argon and nitrogen gas have been connected to the chamber to supply the gas required for the experiment. The amount of gas that flows into the chamber is controlled by gas regulator and a valve for each gas.

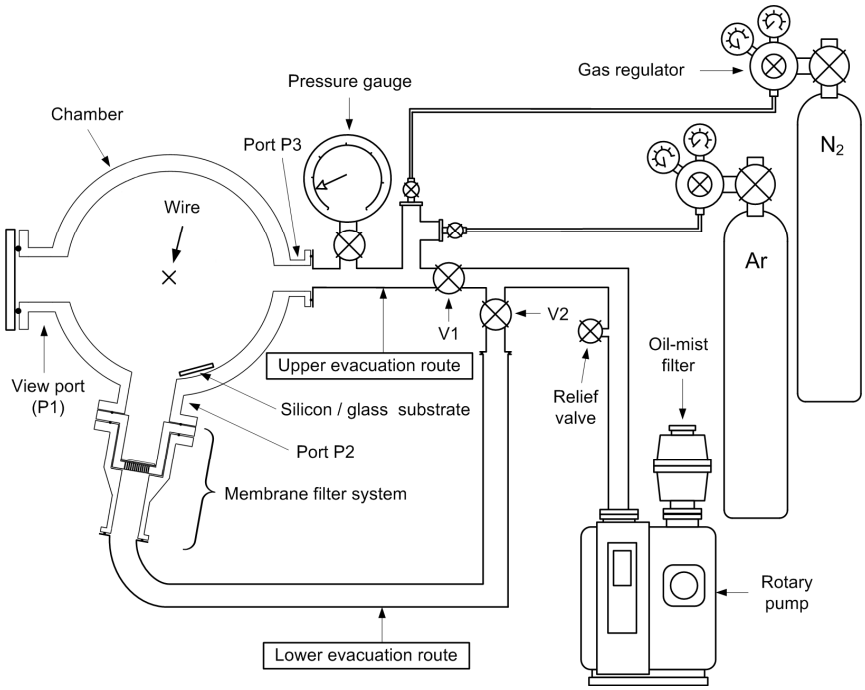

Figure 3.11: The gas and vacuum system.

3.5 Diagnostic tools

3.5.1 Introduction

Three diagnostic tools have been used in this work to obtain the current and voltage across the wire as well as the light emission intensity of the wire explosion. The time-resolved current and voltage waveforms have been obtained by using a magnetic pick-up coil and a high-voltage probe respectively. A PIN diode has been used to measure the intensity of light emitted from the wire explosion. The position of the diagnostic tools along the wire explosion circuit is shown in Figure 3.12. As shown in the figure, the BNC socket of the magnetic pick-up coil has been fastened on the Earth plate to fix the position of the coil. Besides that, the coil is covered by a PVC tube to protect the coil. The tip of the high voltage probe has been attached to the upper spark gap electrode while its ground lead is clamped on the supporting rod. Meanwhile, the PIN diode is located in front of the view port to capture the light emitted during the explosion of the wire.

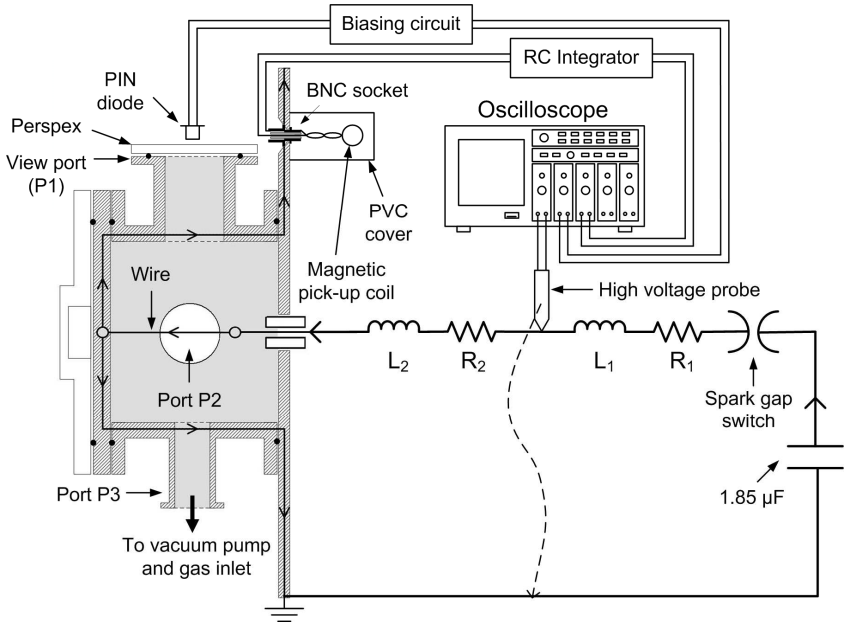

Figure 3.12: Schematic diagram of the wire explosion circuit and the diagnostic tools.

3.5.2 Magnetic pick-up coil and RC integrator

Magnetic field will be induced around a conductor when current is flowing through it. By Ampere's law, the magnitude of the induced magnetic field outside a cylindrical conductor with radius R is given by:

$$B = \frac{\mu_o I}{2\pi r} \tag{3.1}$$

where μ_o = permeability of free space = $4\pi \times 10^{-7}$ H m^{-1},

I = discharge current,

r = perpendicular distance from the axis of the cylindrical conductor (> R).

Meanwhile, the magnetic flux through a surface with an area A is defined as:

$$\Phi_B = AB \cos \varphi \tag{3.2}$$

where A = total surface area cross by the magnetic flux,

B = magnitude of magnetic field,

φ = the angle between the direction of magnetic field and a line perpendicular to the surface.

From the Faraday's law of induction, the electromotive force (emf) induced in a closed loop equals to the negative of the rate of change of magnetic flux through the loop:

$$V = -\frac{d\Phi_B}{dt} \tag{3.3}$$

where V = the induced emf,

Φ_B = the magnetic flux.

If we have a coil with N identical turns and Φ_B is the flux through each turn, then the total emf induced in this coil will be given by:

$$V = -N\frac{d\Phi_B}{dt} \tag{3.4}$$

A magnetic pick-up coil is a small diameter N turns coil made from insulated copper wire. It measures the discharge current flowing through the wire as well as the plasma based on the above principle. Assume that the magnetic field across each turn of the coil is parallel to the coil's axis as shown in Figure 3.13. From (3.2), the magnetic flux through the coil is $\Phi_B = AB$ since $\varphi = 0$ in this case. When the current in the wire explosion circuit changes in magnitude or direction, the magnetic flux around the wire will change as well. According to Faraday's law, an emf will then be induced across the terminals of the magnetic pick-up coil when the magnetic flux changes.

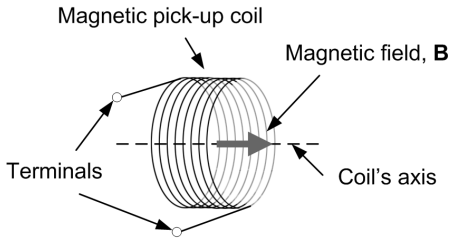

Figure 3.13: Magnetic field crossing the magnetic pick-up coil.

From (3.1), (3.2) and (3.4), the induced emf across the magnetic pick-up coil is given by:

$$\begin{aligned} V &= -N\frac{d\Phi_B}{dt} \\ &= -N\frac{d}{dt}AB \\ &= -NA\frac{d}{dt}\left(\frac{\mu_o I}{2\pi r}\right) \\ &= -\frac{NA\mu_o}{2\pi r}\frac{dI}{dt} \end{aligned} \tag{3.5}$$

The equation shows that the induced emf is proportional to the rate of change of current flowing through the wire. By using a RC integrator, the induced emf across the terminal of the coil can be integrated to give the current flowing through the wire and

plasma. The output of the magnetic pick-up coil will be connected to an oscilloscope through a RC integrator to record the current waveform. Circuit for the RC integrator being used in the experiment is shown in Figure 3.14.

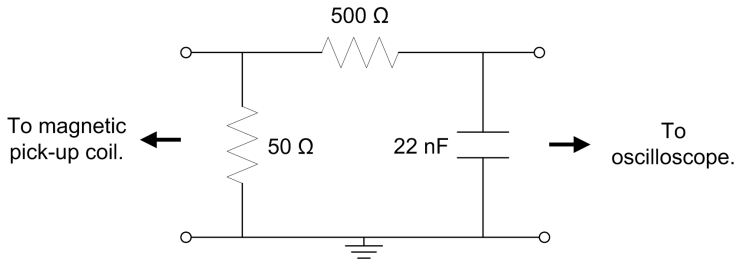

Figure 3.14: RC integrator circuit.

The 50 Ω resistor in the RC integrator is used for impedance matching purpose. Meanwhile, the 500 Ω resistor and the 22 nF capacitor is used to integrate the induced emf across the terminal of magnetic pick-up coil. The measurement of the oscilloscope across the output of the RC integrator will only give a value proportional to the current flow in the wire explosion circuit. In order to obtain the actual magnitude of the current, calibration on the coil output is needed.

3.5.2.1 Calibration of magnetic pick-up coil

By carry out the calibration of the coil, a calibration constant will be deduced. By multiplying the constant with the current data recorded by the oscilloscope, the actual magnitude of current flowing in the circuit can be obtained.

During calibration, the coil will be located at the position where it will be used in the actual experiment. An experimental condition will be chosen such that an ideal LCR discharge is obtained. In this work, an ideal LCR discharge is obtained by connecting the wire holder with a 1 mm diameter insulated copper wire that will not be

exploded by the discharge of the capacitor. A typical current waveform of the ideal LCR discharge is shown in Figure 3.15. In this ideal LCR discharge, no plasma is formed. Thus, the total inductance, $L = L_o + L_w$ where L_o is the inductance of the circuit without wire (or plasma) and L_w is the inductance of the wire. Meanwhile, the total resistance, $R = R_o + R_w$ where R_o is the resistance of the circuit without wire (or plasma) and R_w is the resistance of wire. With the wire as load, L_w and R_w are fixed. On the other hand, with plasma, $L = L_o + L_p(t)$ and $R = R_o + R_p(t)$ where $L_p(t)$ and $R_p(t)$ are the time varying plasma inductance and resistance respectively.

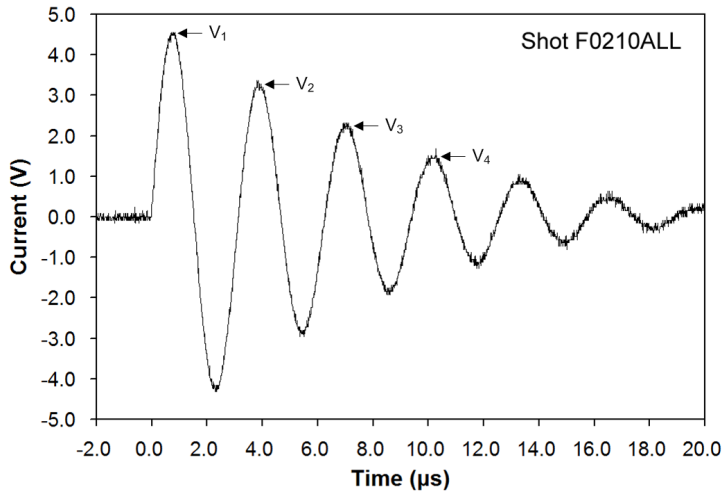

Figure 3.15: Typical current waveform of an ideal LCR discharge of the wire explosion system with fixed load.

The underdamped current waveform can be represented by the expression:

$$I(t) = I_0 e^{-\alpha t} \sin \omega t \tag{3.6}$$

where

$$I_0 = \frac{V_0}{Z_0} \tag{3.7}$$

$$Z_0 = \sqrt{\frac{L}{C}} \tag{3.8}$$

$$\alpha = \frac{R}{2L} \tag{3.9}$$

$$\omega_o = \frac{1}{\sqrt{LC}} = \frac{2\pi}{T} \tag{3.10}$$

$$\omega = \sqrt{\omega_o^2 - \alpha^2} \tag{3.11}$$

I_o, V_o, Z_o, L, C, α, R, ω_o, ω and T representing peak discharge current (without damping), capacitor charging voltage, characteristic impedance, total inductance, capacitance of capacitor, damping factor, total resistance, un-damped resonance frequency, damped resonance frequency and period of current waveform respectively. The un-damped resonance frequency, ω_o, total inductance, L, characteristic impedance, Z_o and discharge current, I_o can be deduced by using the above equations.

From the current waveform shown in Figure 3.15, we can obtain the value for V_1, V_2, V_3, V_4 and the period of the waveform, T. Together with the value of the charging voltage of the capacitor, V_o and the capacitance of the capacitor, C, the calibration constant can be calculated as shown below.

From the measured current waveform, the damping factor is given by:

$$\alpha_n = -\frac{\ln\left(\frac{V_{n+1}}{V_n}\right)}{T} \tag{3.12}$$

Using (3.12), we can get:

$$\alpha_1 = -\frac{\ln\left(\frac{V_2}{V_1}\right)}{T} \quad ; \quad \alpha_2 = -\frac{\ln\left(\frac{V_3}{V_2}\right)}{T} \quad ; \quad \alpha_3 = -\frac{\ln\left(\frac{V_4}{V_3}\right)}{T}$$

Then, the average damping factor is given by:

$$\alpha = \frac{1}{3}(\alpha_1 + \alpha_2 + \alpha_3) \tag{3.13}$$

From (3.9), the circuit resistance, R_o, can be obtained. Meanwhile, the calibration constant, K is given by the equation:

$$K_n = \frac{I_n}{V_n} \tag{3.14}$$

Consider at $t = \frac{T}{4}$, where $I_1 = I_o \exp\left(-\frac{\alpha T}{4}\right)$, then the calibration constant is:

$$K_1 = \frac{I_1}{V_1} = \frac{I_o \exp\left(-\frac{\alpha T}{4}\right)}{V_1}$$

By making use of (3.7), (3.8), (3.10) and (3.12),

$$K_1 = \frac{2\pi C V_o}{T V_1}\left(\frac{V_2}{V_1}\right)^{\frac{1}{4}} \tag{3.15}$$

Similarly, we can obtain K_2 at $t = \frac{5T}{4}$ and K_3 at $t = \frac{9T}{4}$. Finally, the average calibration constant is given by:

$$K = \frac{1}{3}(K_1 + K_2 + K_3) \tag{3.16}$$

The average calibration constant for the magnetic pick-up coil has been determined to be 7.0 kA V^{-1}. The calculated circuit parameters are summarized in Table 3.3.

Table 3.3: Circuit parameters of the wire explosion circuit.

1	Discharge current, I_o	37 kA
2	Characteristic impedance, Z_o	0.27 Ω
3	Total inductance, L	136 nH
4	Total resistance, R	30 mΩ
5	Damping factor, α	1.1 x 10^5 s^{-1}
6	Discharge period, T	3.15 μs

The inductance and the resistance of the insulated copper wire with 1 mm diameter can be calculated from the following expressions:

$$L_w = \frac{\mu_o}{2\pi} \ln\left(\frac{r_{o1}}{r_i}\right) \tag{3.17}$$

$$R_w = \frac{\rho \ell}{A} \tag{3.18}$$

where L_w = wire inductance,

μ_o = permeability of free space,

r_{o1} = radius of the outer conductor (chamber body) = 4.7 cm,

r_i = radius of wire,

ρ = resistivity of the wire at room temperature,

R_w = wire resistance.

They are estimated to be 56 nH and 1.5 mΩ respectively. Subtracting these values from the total inductance and total resistance will allow us to obtain the inductance and resistance for the circuit without wire. In the case here, it is assumed that the change in wire inductance and resistance throughout the discharge process is negligible during the capacitor discharge. Then, the inductance and resistance of circuit without wire are L_o = 80 nH and R_o = 28.5 mΩ respectively.

3.5.3 High voltage probe

A high voltage probe (Tektronix P6015A) with 1000 times attenuation has been used to measure the voltage across the wire. This probe is able to measure a peak pulse of 40 kV. Detail information and specification of the probe can be found in its instruction manual. In order to measure the voltage across the wire, the tip of the probe has to be attached to the upper spark gap electrode.

3.5.4 PIN diode and biasing circuit

A PIN diode is made of a thick intrinsic semiconductor layer sandwiched by a p-type semiconductor and an n-type semiconductor, which is suggested by its name. The model of PIN diode used in the experiment is BPX65. It is able to detect electromagnetic radiation with the wavelength from 350 nm to 1100 nm. The PIN diode will be connected to the oscilloscope through a biasing circuit. The biasing voltage being applied is -45 V. The PIN diode will capture the light emitted from the wire explosion and the intensity of the light will be shown on oscilloscope as a function of time.

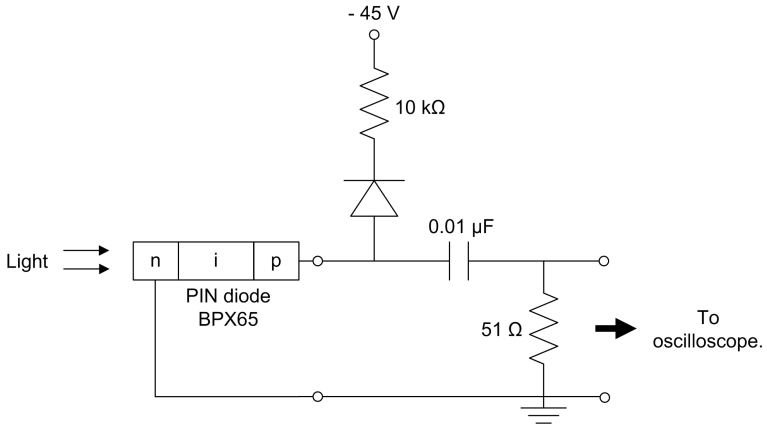

Figure 3.16: PIN diode and biasing circuit.

3.6 Analysis of current, voltage and light emission data

The waveforms of the current, voltage and light emission data obtained by the diagnostic tools and recorded by the oscilloscope will be plotted and analyzed. These data can provide information on the wire explosion process that will allow us to improve the synthesis method and thus the quantity and quality of the nanopowder being synthesized. The current waveform is ready to be analyzed after multiplying the raw data from oscilloscope with the calibration constant. On the other hand, it should be noted that the voltage measured by the voltage probe is not the exact voltage across the wire; it also includes the voltage contributed by other resistive and inductive elements in the circuit (Cho, et al., 2004).

3.6.1 Calculation of deposited energy due to the resistive heating of wire

With the available current and voltage data for a wire explosion, it is possible to deduce the energy deposited into the wire during the resistive heating of the wire before the formation of plasma occurs. This can be done by using the following relation:

$$E(t) = \int I(t) \cdot V_{w,R}(t)\ dt \qquad (3.19)$$

where $E(t)$ = total energy deposited into the wire at time t,

$I(t)$ = time varying current across the wire,

$V_{w,R}(t)$ = time varying voltage across the wire due to the resistive component of the wire,

= $I(t) \cdot R_w$

The voltage across the wire is contributed by both of the wire inductance and resistance as shown in equation (3.20). However, the resistive heating of the wire is only due to the resistive component of the wire. This is the reason for the use of the term $V_{w,R}(t)$ in equation (3.19).

$$V_w(t) = [I(t)\cdot R_w] + [L_w\left(\frac{dI(t)}{dt}\right)] \tag{3.20}$$

By making use of equation (3.20), we have:

$$V_{w,R}(t) = I(t)\cdot R_w = V_w(t) - [L_w\left(\frac{dI(t)}{dt}\right)] \tag{3.21}$$

It is assumed that the wire geometry is approximately the same before the plasma is formed or before the wire is exploded. Hence, the wire inductance L_w will be assumed to be constant in equation (3.21). Then, the value for $V_{w,R}(t)$ can be obtained and the energy deposited into the wire due to resistive heating can be calculated.

3.7 Analysis of powder by TEM, FESEM and XRD

The collected powder is viewed by TEM and FESEM in order to examine the shape and size of particles being produced. From TEM images, size of the nanoparticles being observed will be measured. After that, particle size distribution (PSD) for nanopowder produced from wire explosion in different ambient condition will be constructed. Comparison will be made among the PSD to study the effect of the ambient condition on the PSD.

While the powder will go through some sample preparation processes before being viewed by TEM, powder collected on silicon substrate is viewed directly by using FESEM without any alteration on the sample. Therefore, samples view by FESEM will allow us to observe the original powder as produced from the wire explosion. Besides

that, FESEM allows us to observe micron to submicron size particles more easily compared to that by TEM.

On the other hand, powders collected by glass substrates are analysed by XRD to determine the crystalline structure of the powders. XRD pattern will be obtained from the analysis. If the powders consist of crystal form, sharp peaks corresponding to the crystalline structures will be observed on the XRD patterns. However, if the powders are in the form of amorphous, a broad peak will be observed. The crystal structure corresponding to each crystalline peak can be determined by knowing the value of 2θ corresponding to the peak. After the values of 2θ have been determined, they will be compared with the values in XRD database to identify the crystal structure corresponding to each peak.

3.7.1 Statistical study on the measured particle size

The measured particle sizes from TEM images for each sample will be grouped into 20 classes within the range of 1 nm and 99 nm. The distribution of the measured particle sizes is studied by adopting log-normal distribution function. The log-normal distribution for each sample is obtained by first calculating the geometrical standard deviation and median diameter of the size of particles being measured. The two terms can be obtained from the following equations:

$$\ln \sigma_g = \sqrt{\frac{\sum n_i (\ln d_i - \ln D_{50})^2}{\sum n_i}} \tag{3.22}$$

$$\ln D_{50} = \frac{\sum n_i \ln d_i}{\sum n_i} \tag{3.23}$$

where

σ_g = geometrical standard deviation
D_{50} = median diameter
d = diameter
n_i = number of particle with diameter d_i

After that, the two values will be substituted into equation (3.24) to produce the log-normal distribution.

$$f(d_i) = \frac{1}{\left(\sqrt{2\pi}\right) d_i \ln \sigma_g} \exp\left\{-\frac{\left(\ln d_i - \ln D_{50}\right)^2}{2\left(\ln \sigma_g\right)^2}\right\} \tag{3.24}$$

The log-normal distribution will change when either the geometrical standard deviation or median diameter changes. The geometrical standard deviation will affect the broadness of the distribution while the median diameter will affect the value of diameter where the curve peaks.